Applied Microbiology and Biotechnology (2024) 108:512
https://doi.org/10.1007/s00253-024-13341-w

APPLIED MICROBIAL AND CELL PHYSIOLOGY

Antibacterial mechanism analysis of resveratrol against *Salmonella typhimurium* via metabolomics

Na Wang[1,2,3,4,5] · Cancan Ning[1,3,4] · Zheng Zhao[1,3,4] · Congyan Yang[2,3,4,5] · Hongtao Ren[1,3,5] · Linlin Chen[1,3,4,5] · Qiuying Yu[1,3,4,5] · Gaiping Zhang[2,4,5,6]

Received: 10 December 2023 / Revised: 19 October 2024 / Accepted: 22 October 2024 / Published online: 12 November 2024

Abstract

Salmonella, a common pathogenic bacterium in food, can have a severe impact on food safety and consumer health. At present, *Salmonella* infection is controlled primarily by the use of antibiotics, which creates unsafe factors for food safety. Thus, finding a natural antibacterial agent is highly practical. In this study, resveratrol was screened from 17 kinds of polyphenols, and its inhibitory mechanism and effects on metabolites of *Salmonella typhimurium* were investigated to occur through cell wall and membrane damage and metabolomics analysis. The results revealed that the minimum inhibitory concentration of resveratrol against *S. typhimurium* was 250 μg/mL. After treatment with resveratrol, the lag period of the strain was prolonged, and the cell wall and membrane structure were destroyed. Scanning electron microscopy (SEM) and transmission electron microscopy (TEM) further confirmed that resveratrol induced damage to the cell walls and cell membrane. The metabolic profile of *S. typhimurium* following resveratrol treatment was analysed by gas chromatography−mass spectrometry. In the metabolome evaluation, we screened 23 differentially abundant metabolites, including 11 upregulated and 12 downregulated metabolites. Eight metabolic pathways of *S. typhimurium*, including pathways important for amino acid metabolism and the tricarboxylic acid (TCA) cycle, exhibited significant changes after resveratrol treatment. The verification results of the citric acid content, *cis*-aconitase activity, and ATP content further revealed that the tricarboxylic acid cycle and other related metabolic pathways of *S. typhimurium* were affected. These results could provide a theoretical possibility for the use of resveratrol as a plant-derived bacteriostatic for food safety problems caused by *S. typhimurium*.

Key points

- *The mechanism of bacteriostasis was studied via metabolomics*
- *Resveratrol causes the death of Salmonella by disrupting the cell wall and membrane*

Keywords Resveratrol · *Salmonella typhimurium* · Antibacterial activity · Metabolomics · Mechanism

Introduction

Salmonella belongs to *Enterobacteriaceae*, which is the second largest foodborne pathogen in the world. It can cause food poisoning in humans and animals and has

Na Wang and Cancan Ning contributed equally to this paper.

✉ Qiuying Yu
yuqiuyingzf@163.com

[1] College of Food Science and Technology, Henan Agricultural University, Zhengzhou 450002, China

[2] College of Animal Medicine, Henan Agricultural University, Zhengzhou 450002, China

[3] Key Laboratory of Nutrition and Healthy Food of Zhengzhou, Zhengzhou 450002, China

[4] International Joint Research Center for Animal Immunology, Zhengzhou 45002, China

[5] Longhu Laboratory of Advanced Immunology, Zhengzhou 450000, China

[6] School of Advanced Agricultural Sciences, Peking University, Beijing 100871, China

important public health significance (Olaimat and Holley 2012; Scallan et al. 2011; Simon et al. 2018; Wang et al. 2019a, b). According to incomplete statistics, 70–80% of outbreaks of foodborne bacteria are caused by *Salmonella* in China (Renoz et al. 2015). *Salmonella typhimurium* is the main serotype causing food poisoning in humans and animals (Ebani et al. 2019; Mezal et al. 2013). Currently, the main treatment for diseases caused by *S. typhimurium* is antibiotic therapy (Diard et al. 2014). Because of the extensive use and abuse of antibiotics, multidrug resistance in *S. typhimurium* is gradually increasing, thus greatly increasing the difficulty of preventing and treating *S. typhimurium* (Deng et al. 2018). For example, common antibiotics such as cephalosporins and kanamycin have reduced the actual therapeutic effect. Studies have shown that plant polyphenols have natural, nontoxic side effects and other advantages in the prevention and treatment of foodborne diseases. This emerging microecological therapy has become a research hotspot.

Polyphenols are a general term for compounds containing multiple phenolic hydroxyl groups and their derivatives, including flavonoids, phenolic acids, stilbenes, coumarins and tannins. Current studies have confirmed that polyphenols in plants have antibacterial properties. Stojković et al. (2013) determined the antibacterial activities of coumaric acid, caffeic acid and rutinum in chicken soup. The study revealed that coumaric acid (> 0.1 mg/mL), caffeic acid (> 0.1 mg/mL) and rutinum (> 0.9 mg/mL) completely inhibited the growth of *Staphylococcus aureus* in chicken soup (25 and 4 °C). Li et al. (2020) reported that resveratrol at 0.8 mg/mL completely inhibited the growth of *Streptococcus mutans*. Resveratrol, an important phenolic acid, has attracted widespread attention for its anti-inflammatory, antibacterial, antioxidant, glucose regulatory, lipid metabolism and antiaging properties (Biasutto et al. 2017; Singh and Vinayak 2016; Singh et al. 2019). Marino et al. (2013) reported that the anti-inflammatory effect of resveratrol had an inhibitory effect on keratitis caused by *S. aureus* infection. Duan et al. (2018) reported that resveratrol reduced the virulence of *S. aureus* by downregulating the production of the sae RS α-haemolysin, which also inhibited the haemolytic capacity of *S. aureus*. However, the antibacterial activities of resveratrol against *S. typhimurium*, as well as the underlying mechanisms, have received little attention.

In this study, we determined the inhibition zone diameter (DIZ), minimum inhibitory concentration (MIC) and effect of resveratrol on the growth curve of 17 polyphenols. The antibacterial mechanism was studied by measuring the cell wall integrity, membrane permeability and biofilm formation capacity and by using scanning electron microscopy (SEM) and transmission electron microscopy (TEM). Furthermore, gas chromatography–mass spectrometry (GC–MS) data were used to carry out multivariate statistical analysis and metabolic pathway analysis to determine and analyse the metabolomics of *S. typhimurium* at the MIC to further demonstrate the antibacterial mechanism. This research could provide a theoretical basis for the prevention and control of *S. typhimurium* infection in food industries, such as food-processing environments.

Materials and methods

Experimental materials

Trans-resveratrol, syringic acid, chlorogenic acid, ferulic acid, caffeic acid, protocatechuic acid, phloridin, puerarin, kaempferol, apigenin, gallic acid, rutinum, catechin, epicatechin, quercetin, coumaric acid (≥ 98% purity) and procyanidins (≥ 95% purity) were purchased from China Beijing Solarbio Co. Ltd. Assay kits for alkaline phosphatase, sodium, potassium, magnesium, total protein, ATP, citric acid content and aconitase activity were obtained from China Beijing Solarbio Co. Ltd.

Strains and cultures

The *S. typhimurium* standard strain (ATCC14028) was obtained from the American Strain Collection Center. The strain was inoculated into LB broth for activation and cultured overnight in a 37 °C incubator for 24 h. The bacterium was grown until growth was maintained in the stable phase and then stored for later use.

Screening of the antimicrobial activity of polyphenols against S. typhimurium

Determination of the DIZ

The inhibitory activity was determined according to the agar diffusion method of Guanlin and Jinhua (2006). Two hundred microlitres of a 1×10^6 CFU (colony-forming unit)/mL bacterial suspension was pipetted onto LB agar medium and spread. The wells were punched with a 10-mm diameter puncher, and 200 µL of 10 mg/mL polyphenols was added to each well. While the blank control group (CK) was set up, 2% dimethyl sulfoxide (DMSO) was used as the negative control group (NC), and 62.5 µg/mL kanamycin sulfate was used as the positive control group (PC). The agar plates were incubated at 37 °C for 24 h, and the DIZ was accurately measured.

Determination of the MIC

The MIC was measured by the broth microdilution method (Koch et al. 2019). A 1 mg/mL polyphenol solution was

diluted in LB broth by the twofold dilution method, the final concentration of the polyphenol solution was 3.906 ~ 500 μg/mL, and 100 μL of each mixture was added to a 96-well plate. The bacterial mixture was subsequently diluted to 1×10^6 CFU/mL in LB broth, and 100 μL from each well was added to new 96-well cell culture plates with different concentrations of polyphenol solution. One hundred microlitres of 2% DMSO solution which was safe for the growth of bacteria according to the pretest results, 100 μL of 62.5 μg/mL kanamycin sulfate solution and 100 μL of sterile water were used as the NC, PC and CK, respectively. All the 96-well cell culture plates were stored at 37 °C for 24 h, and the absorbance value at 600 nm was recorded. The lowest concentration corresponding to the sterile growth wells was used as the MIC (Weerakkody et al. 2010). The inhibition rate (X) was calculated via Eq. (1) as follows:

$$X = \left(\frac{C - B}{C - A}\right) \times 100\% \quad (1)$$

A Value of the absorbance of the positive control.
B Value of the absorbance of the experimental group.
C Value of absorbance of the negative control.

Growth curve

Five millilitres of bacterial mixture with a concentration of 1×10^6 CFU/mL was added to each test tube, 5 mL of different resveratrol concentrations (0, 1/4×, 1/2× or 1×MIC) was added and the final volume was 10 mL. Moreover, the NC group and PC group were established. The test tubes were then placed in a shaker at 37 °C and 160 rpm, after which the absorbance at $OD_{600\ nm}$ was measured every 2 h to determine the degree of cell growth within 36 h (Liu et al. 2017).

Assessment of cell wall and cell membrane damage

Alkaline phosphatase activity

The bacteria were cultured with LB broth at 37 °C until they reached the logarithmic stage. The bacterial mixture was removed and centrifuged at 5000 rpm for 10 min, after which the supernatant was discarded. The precipitate was washed with sterile water three times and resuspended to 1×10^6 CFU/mL. Different concentrations of resveratrol (0, 1/4×, 1/2× and 1×MIC) were added to a final volume of 10 mL. The mixture was then placed in a shaker at 37 °C and 160 rpm for 3 h, and the supernatant was collected after the bacterial mixture was centrifuged at 5000 rpm for 10 min. The alkaline phosphatase (AKP) activity was determined according to the method of the AKP test kit (Xu et al. 2016).

Measurement of the cell membrane potential

The membrane potential was analysed by the rhodamine 123 fluorescence staining method (Novo et al. 1999). The bacteria were cultured with LB broth at 37 °C until they reached the logarithmic stage. The bacterial solution was removed and centrifuged at 5000 rpm for 10 min, after which the supernatant was discarded. The precipitate was washed with 0.1 M phosphate buffer (PBS) three times and then resuspended to 1×10^6 CFU/mL. Different concentrations of resveratrol (0, 1/4×, 1/2× and 1×MIC) were added to a final volume of 10 mL. The mixture was then placed in a shaker at 37 °C and 160 rpm for 3 h, and the supernatant was collected after the bacterial solution was centrifuged at 5000 rpm for 10 min. Rhodamine 123 (20 μL) was added to the resuspension mixture (10 mL) to a final concentration of 2 μg/mL. The mixture was incubated for 30 min in the dark and washed with PBS three times after centrifugation, after which the fluorescence value was measured.

Determination of electrical conductivity

The bacteria were cultured with LB broth at 37 ℃ until they reached the logarithmic stage. The bacterial solution was removed and centrifuged at 5000 rpm for 10 min, after which the supernatant was discarded. The precipitate was washed with 0.1 M PBS three times and then resuspended to 1×10^6 CFU/mL. Different concentrations of resveratrol (0, 1/4×, 1/2× and 1×MIC) were added to a final volume of 10 mL. The mixture was then placed in a shaker at 37 °C and 160 rpm for 3 h, and the supernatant was collected after the bacterial mixture was centrifuged at 5000 rpm for 10 min. The conductivity was measured according to the instructions of a conductivity meter (Diao et al. 2014).

Measurement of extracellular Na+, K+ and Mg2+ leakage

The bacteria were cultured with LB broth at 37 ℃ until they reached the logarithmic stage. The bacterial solution was removed and centrifuged at 5000 rpm for 10 min, after which the supernatant was discarded. The precipitate was washed with 0.1 M PBS three times and then resuspended to 1×10^6 CFU/mL. Different concentrations of resveratrol (0, 1/4×, 1/2× and 1×MIC) were added to a final volume of 10 mL. The mixture was then placed in a shaker at 37 °C and 160 rpm for 3 h, and the supernatant was collected after the bacterial solution was centrifuged at 5000 rpm for 10 min. The extracellular Na^+, K^+ and Mg^{2+} mass concentrations were determined by using the appropriate kit methods (Niven et al. 1999; Wang et al. 2014).

Measurement of extracellular protein leakage

The bacteria were cultured with LB broth at 37 ℃ until they reached the logarithmic stage. The bacterial solution was removed and centrifuged at 5000 rpm for 10 min, after which the supernatant was discarded. The precipitate was washed with 0.1 M PBS three times and then resuspended to 1×10^6 CFU/mL. Different concentrations of resveratrol (0, 1/4×, 1/2×and 1×MIC) were added to a final volume of 10 mL. The mixture was then placed in a shaker at 37 °C and 160 rpm for 3 h, and the supernatant was collected after the bacterial mixture was centrifuged at 5000 rpm for 10 min. The bacterial supernatants were subsequently filtered through 0.22-μm Millipore filters (Millipore, Burlington, MA, USA). The content of extracellular protein was tested according to the methods of a BCA kit (Wang et al. 2019a).

Assay for leakage of nucleic acids

Nucleic acid leakage was detected using a previously described method (Lv et al. 2011). The bacteria were cultured with LB broth at 37 ℃ until they reached the logarithmic stage. The bacterial mixture was removed and centrifuged at 5000 rpm for 10 min, after which the supernatant was discarded. The precipitate was washed with 0.1 M PBS three times and then resuspended to 1×10^6 CFU/mL. Different concentrations of resveratrol (0, 1/4×, 1/2×and 1×MIC) were added to a final volume of 10 mL. The mixture was then placed in a shaker at 37 °C and 160 rpm for 3 h, and the supernatant was collected after the bacterial solution was centrifuged at 5000 rpm for 10 min. The absorbance was measured at a wavelength of 260 nm.

Determination of biofilm formation

The biofilms of the strains were analysed using a previously reported method (Vasudevan et al. 2003). The bacterial suspension was cultured to the logarithmic growth phase and diluted to 1×10^6 CFU/mL with LB broth. Different concentrations of resveratrol (0, 1/4×, 1/2×and 1×MIC) were added, and the mixture was then placed in a shaker for 24 h at 37 °C to allow the cells to attach to the 96-well plates. Afterwards, planktonic cells were removed, and each well was washed three times. The wells were fixed with 200 μL of 40% formaldehyde for 15 min and stained with 1% crystal violet solution for 5 min to colour the biofilms. They were then washed with PBS three times, the crystal violet was dissolved and the coloured biofilm was released after 200 μL of 33% acetic acid was added. The samples were then incubated at 37 °C for 30 min, after which the absorbance at OD_{590nm} was measured.

SEM and TEM observations

The bacteria were cultured with LB broth at 37 ℃ until they reached the logarithmic stage. The bacterial solution was removed and centrifuged at 5000 rpm for 10 min, after which the supernatant was discarded. The precipitate was washed with 0.1 M PBS three times and then resuspended to 1×10^6 CFU/mL. Different concentrations (0, 1/4×, 1/2×and 1×MIC) of resveratrol were added to the medium, and then the mixture was placed in a shaker at 37 °C for 3 h. All the samples were centrifuged at 8000 rpm for 8 min, and the supernatant was discarded. The bacteria were fixed overnight at 4 °C with 4% glutaraldehyde solution after they were washed with PBS three times. The samples were subsequently gradient eluted for 15 min with ethanol solutions (30%, 50%, 70%, 80%, 90% and 95%). They were then treated with anhydrous ethanol. The samples were dried in a critical point dryer, and the bacteria was removed for gold spraying for observation and image acquisition (Yi et al. 2016).

The bacterial pretreatment for TEM was the same as that for SEM. The bacteria were fixed overnight at 4 °C with 4% glutaraldehyde solution after washing with PBS three times. All the samples were fixed with 1% osmic acid at 4 °C for 3 h. After step-by-step dehydration with acetone solutions and drying, the samples were embedded with an embedding agent, polymerised to make ultrathin sections, and then stained with uranyl acetate. Images were collected after drying and then observed under a transmission electronic microscope (Hyldgaard et al. 2014).

Metabolomics

S. typhimurium was inoculated in LB liquid medium and cultured to the logarithmic stage at 37 °C. The bacteria were collected after centrifugation (8000 rpm, 10 min). They were then resuspended in fresh LB liquid medium, and resveratrol was added to a final concentration of 250 μg/mL (MIC) as the test group (T). The bacteria were cultured at 37 °C for 3 h, centrifuged at 8000 rpm for 10 min, washed three times with sterile 0.01 M PBS (pH 7.4) and frozen in a refrigerator at − 80 °C until use.

After sample preparation, pretreatment, intracellular metabolite extraction, GC–MS, full-scan detection, data pretreatment and statistical analyses were performed by Shanghai Meiji Biological Co., Ltd. Metabolomic-data-processing software Progenesis OI Mass Hunter Workstation Quantitative Analysis (Agilent, Santa Clara, CA, USA) was used for standardised preprocessing. Multivariate statistical analysis and method enrichment were then carried out on standardised peak areas (Liu et al. 2020). A combination of multidimensional analysis and single-dimensional analysis was used to screen different metabolites between

groups (Westerhuis et al. 2010). In the analysis of orthogonal projections to latent structures discriminant (disturbance), the variable importance in projection (VIP) represents the importance of the variable to the entire model and is the weighted sum of squares (Dan et al. 2021). Metabolic pathway enrichment analysis of the differentially abundant metabolites was performed via the Kyoto Encyclopedia of Genes and Genomes (KEGG) database (https://www.kegg.jp/kegg/). The KEGG IDs of the different metabolites were used to conduct pathway enrichment analysis to obtain the enrichment results of the metabolic pathways and to determine the metabolic pathways with significant differences between the strains after treatment with resveratrol.

Determination of citric acid content, cis-aconitase activity and ATP content

The bacteria were cultured with LB broth at 37 ℃ until they reached the logarithmic stage. The bacterial solution was removed and centrifuged at 5000 rpm for 10 min, after which the supernatant was discarded. The precipitate was washed with 0.1 M PBS three times and then resuspended to 1×10^6 CFU/mL. Different concentrations of resveratrol (0, 1/4×, 1/2×and 1×MIC) were added to a final volume of 10 mL. The mixture was then placed in a shaker at 37 °C and 160 rpm for 3 h and centrifuged first to separate the bacteria from the supernatant. The collected bacteria were then suspended by adding the corresponding reagents of the kits and placed on ice for ultrasonic crushing (300-W power, 3-s ultrasonication, 9-s interval, and 4-min total time). The samples were centrifuged, and the supernatants were collected. The contents of citric acid and intracellular ATP, as well as the activity of *cis*-aconitase, were determined with the relevant kits.

Statistical analysis

All experiments were performed in parallel three times for each group. Statistical analysis was performed via SPSS software (IBM, SPSS Inc., Chicago, IL, USA). The data is expressed as the means ± standard deviations ($n = 3$). Differences among multiple groups were compared by one-way ANOVA. The differences were considered significant at $P < 0.05$.

Results

Screening of the antimicrobial activity of polyphenols against S. typhimurium

Figure 1 shows the antibacterial effects of 17 polyphenol compounds. Significant inhibition activity was presented by coumaric acid, resveratrol, caffeic acid, gallic acid, ferulic

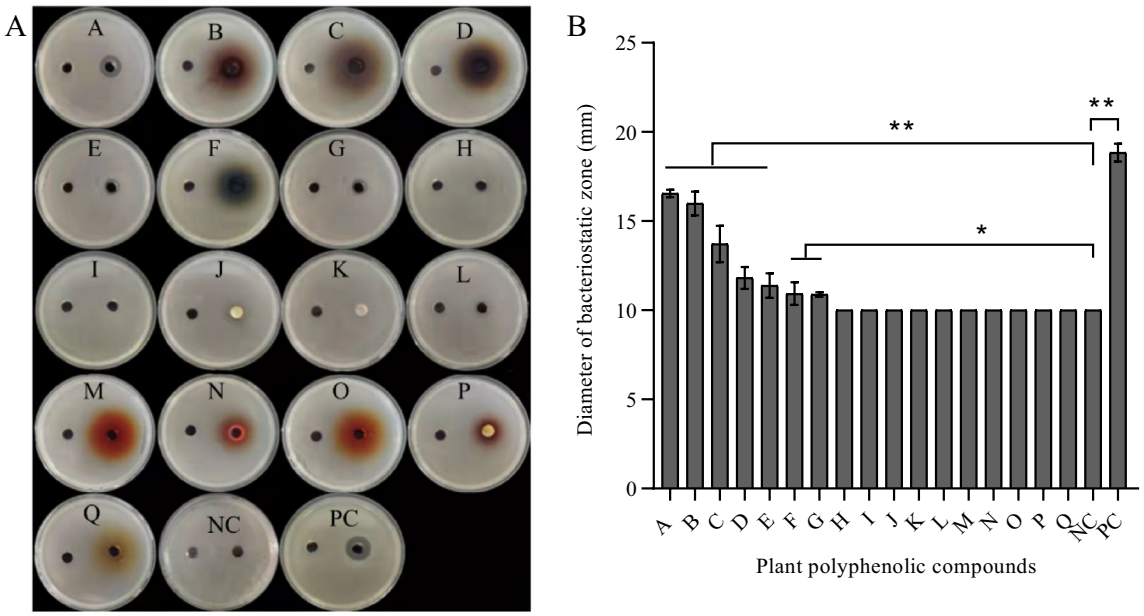

Fig. 1 Antibacterial effect of plant polyphenols on *S. typhimurium* as analysed by agar diffusion tests. (**A**) Photographs of selected plates with empty wells to the left and wells filled with test substances to the right after 24 h growth at 37 ℃. (A) Coumaric acid. (B) Resveratrol. (C) Caffeic acid. (D) gallic acid. (E) Ferulic acid. (F) Protocatechuic acid. (G) Chlorogenic acid. (H) Clove acid. (I) Phlorizin. (J) Kaempferol. (K) Apigenin. (L) Puerarin. (M) Epicatechin. (N) Proanthocyanidin. (O) Catechins. (P) Quercetin. (Q) Rutinum. Plate NC: negative control. Plate PC: positive control. **B**. Measurements in mm of the inhibition zones as generated around wells in agar plates by addition of respective test substances (* means $P < 0.05$; ** means $P < 0.01$)

acid, protocatechuic acid, and chlorogenic acid (Fig. 1(A)). Compared with those in the NC group, the contents of coumaric acid, resveratrol, caffeic acid, gallic acid, and ferulic acid were significantly different ($P < 0.01$), with DIZ values of 16.56, 15.99, 13.71, 11.82, and 11.38 mm, respectively. The contents of protocatechuic acid and chlorogenic acid significantly differed ($P < 0.05$), with DIZ values of 0.94 and 10.89 mm, respectively (Fig. 1(B)).

The MICs of the seven polyphenol compounds are shown in Fig. 2. The MICs of coumaric acid and resveratrol against *S. typhimurium* were 500 and 250 μg/mL, respectively (Fig. 2A and B). The antibacterial rates are displayed in Table 1. The antibacterial rates of resveratrol and coumaric acids were 96.53% and 22.63%, respectively, when the concentration was 250 μg/mL.

Growth curve

To further explore the antibacterial activity of resveratrol, the course of growth of *S. typhimurium* in the presence

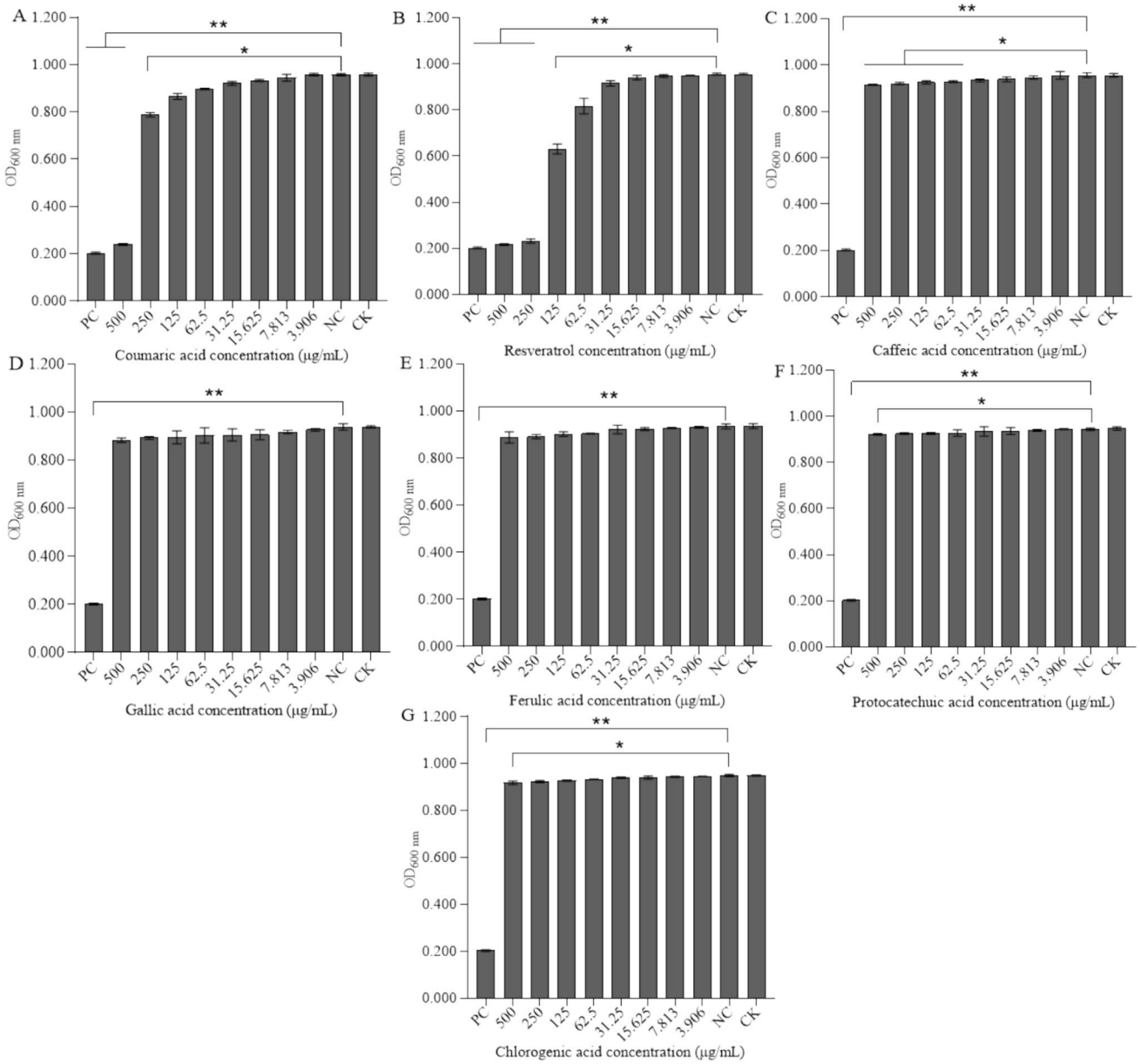

Fig. 2 Minimum inhibitory concentration of different plant polyphenols on *S. typhimurium* as measured after 24 h incubation at 37 ℃ of each 1×10^6 CFU/mL cultivated in 200 uL LB medium plus respective additions in wells of 96-well microplates. **A** Coumaric acid. **B** Resveratrol. **C** Caffeic acid. **D** Gallic acid. **E** Ferulic acid. **F** Protocatechuic acid. **G** Chlorogenic acid. Abbreviations used are NC for negative control, PC for positive control, and CK for untreated cells. (* means $P < 0.05$; ** means $P < 0.01$)

Table 1 Antibacterial rate of plant polyphenols against *S. typhimurium* (% of inactivation)

Name	Concentration (μg/mL)							
	500	250	125	62.5	31.25	15.625	7.813	3.906
Resveratrol	97.97 ± 0.64	96.54 ± 0.27	43.28 ± 1.78	18.54 ± 3.56	5.35 ± 0.98	2.10 ± 0.78	1.43 ± 0.53	1.37 ± 0.44
Coumaric acid	95.11 ± 0.09	22.64 ± 0.78	12.29 ± 0.85	8.02 ± 0.36	4.93 ± 0.38	3.28 ± 0.32	2.32 ± 0.61	0.18 ± 0.13
Caffeic acid	5.31 ± 0.53	4.66 ± 0.59	4.09 ± 0.24	3.60 ± 0.47	2.89 ± 0.52	2.37 ± 0.73	1.72 ± 0.83	0.27 ± 0.01
Gallic acid	7.59 ± 0.64	6.27 ± 0.30	5.91 ± 2.55	4.86 ± 1.13	4.55 ± 0.83	4.46 ± 0.91	3.93 ± 0.73	3.34 ± 0.48
Ferulic acid	6.51 ± 0.98	6.07 ± 0.34	4.66 ± 0.27	4.20 ± 0.99	1.92 ± 0.99	1.55 ± 0.54	1.43 ± 0.42	1.26 ± 0.97
Chlorogenic acid	4.15 ± 0.60	3.54 ± 0.27	2.87 ± 0.25	2.15 ± 0.17	1.26 ± 0.24	1.12 ± 0.53	0.96 ± 0.08	0.93 ± 0.35
Protocatechuic acid	3.40 ± 0.42	2.91 ± 0.71	2.83 ± 0.36	2.66 ± 0.76	1.62 ± 0.78	1.50 ± 0.89	1.28 ± 0.66	0.74 ± 0.56

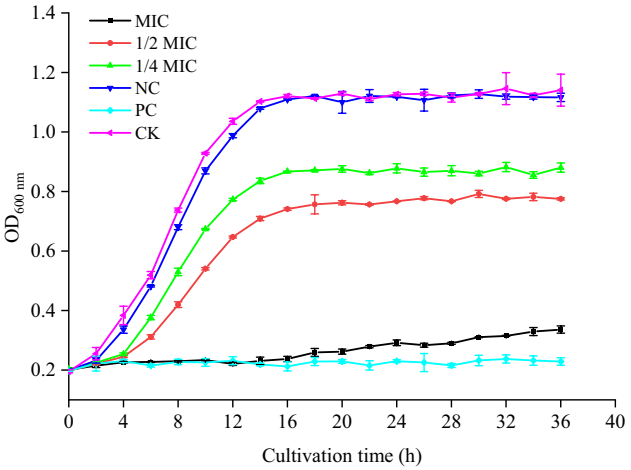

Fig. 3 Growth curve of *S. typhimurium* cultivated in 10 mL LB medium in sterile test tubes at 37 ℃ under the inhibition of resveratrol at different concentrations. Abbreviations used: NC, negative control; PC, positive control; CK, blank control

of different concentrations of resveratrol was plotted. The growth curve of the bacteria was S shaped (Fig. 3). Resveratrol at 1/4 × and 1/2 × MIC presented better inhibitory effects on the growth of *S. typhimurium*. However, when the concentration of resveratrol was 1 × MIC, the growth of *S. typhimurium* was almost completely inhibited.

Effect of resveratrol on the cell wall and cell membrane of S. typhimurium

As shown in Fig. 4A, the AKP activity of *S. typhimurium* without resveratrol treatment displayed no obvious changes. However, the amount of AKP in the culture medium exhibited a significant increase after treatment with resveratrol (1/4 ×, 1/2 × and 1 × MIC).

The damage caused by resveratrol to the cell membrane of *S. typhimurium* was reflected in the membrane potential, conductivity and leakage rates of Na^+, K^+ and Mg^{2+}, as well as the protein and nucleic acid contents. In contrast to those in the CK group, the membrane potential, conductivity and leakage rates of Mg^{2+} and the nucleic acid content were significantly different at resveratrol concentrations of 1/4 ×, 1/2 × and 1 × MIC (Fig. 4B, C, F, H). The leakage rates of Na^+ and K^+ and the protein content significantly increased when the resveratrol concentration was at 1/2 × or 1 × MIC ($P < 0.01$) (Fig. 4D, E, G). These results confirmed that with the addition of resveratrol, the structures of the *S. typhimurium* cell wall and cell membrane were destroyed, and the protection of the cells was lost, resulting in impaired metabolism.

Antibiofilm activity

A biofilm refers to an organized group of strains attached to the surface of objects that are coated with the extracellular macromolecules of the strains (Lewandowski et al. 2007). A stable internal environment was constructed by the biofilm for the life activities of the cells. Figure 5 shows that compared with that of the control group, the biofilm formation of the 1/2 ×, 1/4 × and 1 × MIC groups was significantly lower ($P < 0.01$), confirming that resveratrol was able to inhibit the formation of biofilms and reduce the metabolic activity of *S. typhimurium* biofilms. Finally, the protective barrier of *S. typhimurium* was depleted, and its invasive ability was weakened. This effect was similar to the inhibitory effect of *Dodartia orientalis* L. essential oil on the biofilm formation of *Salmonella enteritidis* reported by Wang et al. (2017).

SEM and TEM analysis

SEM and TEM are powerful tools for further investigating the effects of resveratrol on bacterial cells and play important roles in observing the morphological and ultrastructural changes in *S. typhimurium* treated with resveratrol (Fig. 6), similarly as described before for the species and other food-pathogenic bacteria (Chen et al. 2017). As shown in Fig. 6(a) and (A), SEM revealed that the *S. typhimurium* cells in the control group presented a regular short rod shape and smooth surface, the cell structures observed using TEM were complete and the cell aggregates were dense and evenly

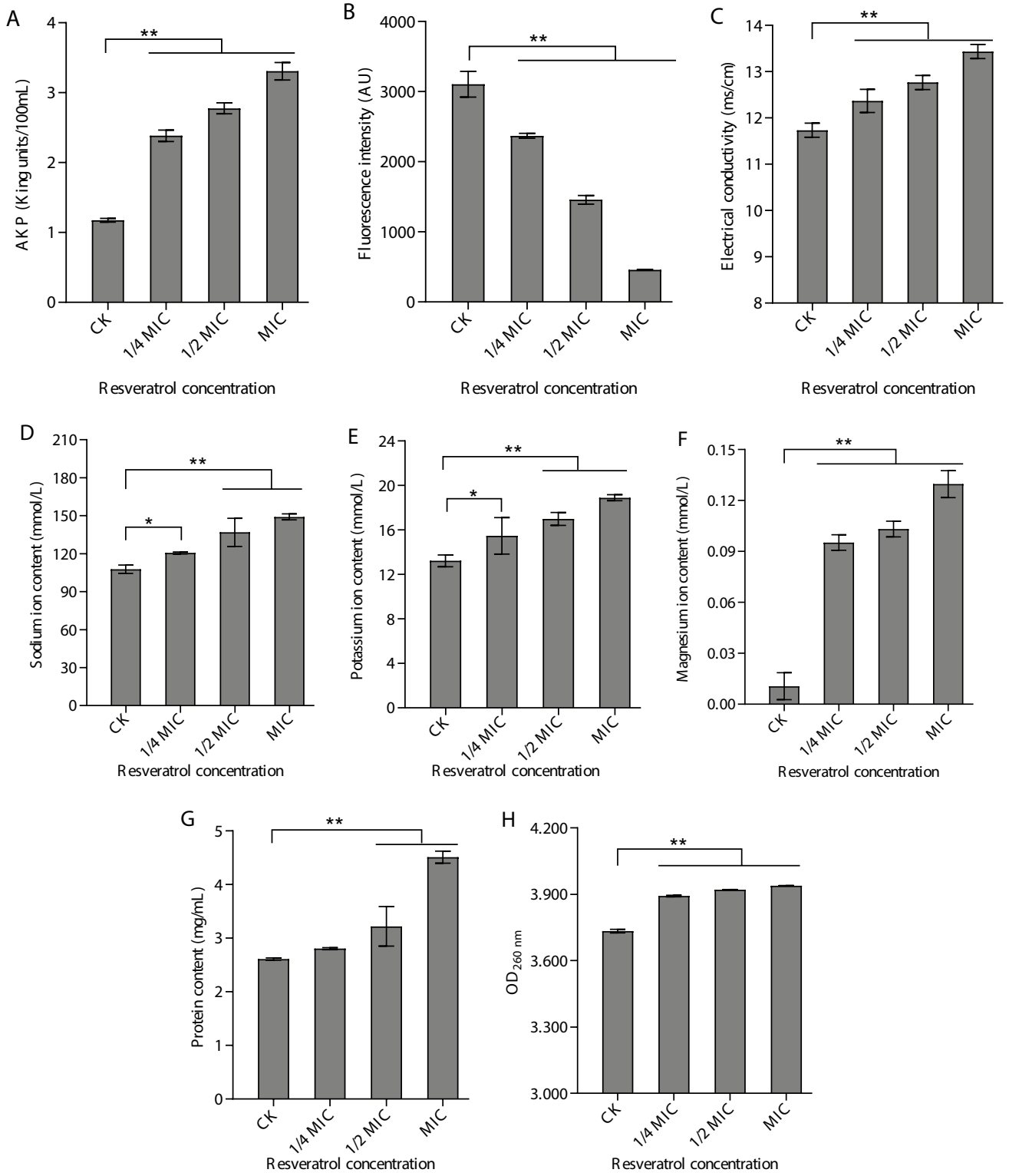

Fig. 4 Effect of resveratrol on cell walls and cell membrane in *S. typhimurium*. **A** Release of intracellular alkaline phosphatase activity. **B** Membrane potential. **C** Conductivity. **D** Na^+ leakage. **E** K^+ leakage. **F** Mg^{2+} leakage. **G** Protein leakage. **H** Nucleic acid leakage. Abbreviations used: CK, blank control. (* means $P < 0.05$; ** means $P < 0.01$)

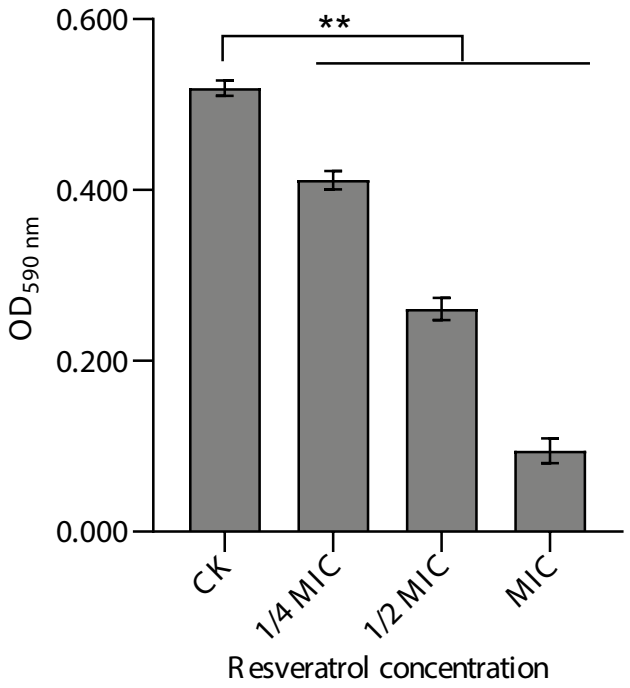

Fig. 5 Effect of resveratrol at different concentrations on biofilm forming ability of *S. typhimurium* as measured after 24 h incubation at 37 ℃ in 96-well cell culture plates. Abbreviations used: CK, blank control. (* means $P<0.05$; ** means $P<0.01$)

distributed. However, when *S. typhimurium* cells were treated with 1/4 ×, 1/2 × or 1 × MIC resveratrol, distorted membrane morphology, leakage of cell contents, an irregularly wrinkled and coarse outer surface and structural damage to parts of the bacterial cells were observed, as shown in Fig. 6(b–d), similarly as previously observed with other bacteria in antimicrobial treatments (Hameed et al. 2016). Some cell walls disappeared, and TEM images revealed cell membrane rupture, cell deformation, and leakage of intracellular substances. There were some cells that were abnormal in morphology and eventually broke down (Fig. 6(B–D)), similarly as observed in antibacterial treatment of *Enterococcus faecalis* (Cao et al. 2019). Patra et al. (2016) reported that the cell membrane structure of *S. typhimurium* became severely damaged after treatment with pyrolytic oil, resulting in irregular folds and a rough outer surface. Similar studies have also shown that the cell membrane structure of *Listeria monocytogenes*, *S. aureus*, *S. enteritidis* and *Vibrio parahaemolyticus* treated with 1 × MIC anthocyanins from blueberries for 2 h changed significantly, as observed via SEM (Sun et al. 2018).

Metabolomic analysis

GC–MS was used to determine the intracellular metabolites so that the antibacterial mechanism of resveratrol against *S. typhimurium* could be measured further. The overall distribution among samples and the stability and reliability of the entire analysis process were determined by using

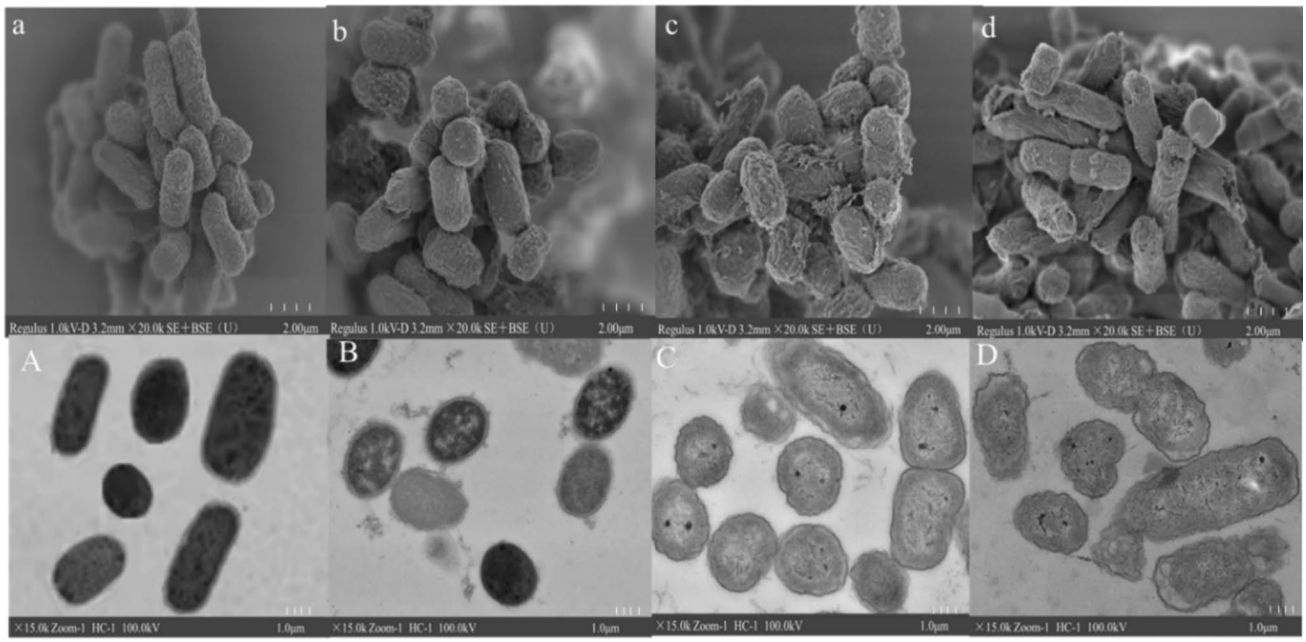

Fig. 6 Scanning electron microscope and transmission electron microscope observation results of *S. typhimurium* treated with resveratrol. (**a** and A) Untreated cells; (**b** and B) Treated with resveratrol at 1/4 × MIC; (**c** and C) Treated with resveratrol at 1/2 × MIC; (**d** and D) Treated with resveratrol at 1 × MIC

multivariate statistics of intracellular metabolites via unsupervised principal component analysis (PCA) and orthogonal partial least-squares discrimination analysis (OPLS-DA). As shown in Fig. 7, the samples treated with and without resveratrol were completely separated and distinguished by PCA and OPLS-DA score evaluation, indicating that resveratrol caused significant changes in the metabolite profile of *S. typhimurium*.

In the heatmap and cluster analysis, the rationality and intuitiveness of relationships among the samples and the changes in metabolite expression patterns among the different samples were reflected. With VIP > 1 and $P < 0.05$ as criteria, 23 metabolites with significant differences were screened. These genes were visualised using volcano plot analysis (Fig. 8A). Cluster analysis revealed that the expression levels of 11 and 12 metabolites, which were regarded as target metabolites, were significantly upregulated and downregulated, respectively (Fig. 8B). The metabolites that presented significant changes involved mainly amino acids and carbohydrates, which are closely related to the disturbance of metabolic pathways such as biosynthesis of the amino acids, organic acids and oxidative phosphorylation.

According to further analysis of the KEGG database, 20 metabolic pathways were influenced in *S. typhimurium* treated with resveratrol (Fig. 9A). In addition, eight of them were key metabolic pathways with impact values (> 0.02) as the reference threshold; in particular, amino acid metabolism and the tricarboxylic acid cycle (TCA cycle) pathway were the main metabolic pathways (Fig. 9B).

Compared with those in the CK group, the expression levels of γ-aminobutyric acid, malonic acid and putrescine in the T group were significantly decreased. γ-Aminobutyric acid is involved in many metabolic pathways, such as arginine and proline metabolism, alanine metabolism, aspartic acid and glutamate metabolism, and β-alanine metabolism. These pathways play important roles in energy and nutrient supply in organisms, peptidoglycan synthesis, protein aggregation, the stability of cell walls and cell membranes, and the regulation of steroid hormones (Ding et al. 2011; Liang et al. 2014; Natera et al. 2006; Takagi et al. 1997; Wu et al. 1993). Pyrimidine is an essential component of nucleotide synthesis, and its metabolism is closely related to changes in malonic acid expression, which directly affects the synthesis of bacterial nucleic acids (West et al. 1982). Changes in the content of putrescine play a crucial role in cell pH, causing an acid–base imbalance in cells and subsequently promoting cell death in *S. typhimurium* (Fig. 9C) and other bacteria (Del Rio et al. 2016). As shown in Fig. 9C, the expression levels of fumaric acid, citric acid, D-malic acid and cyanate in the T group were significantly greater than those in the CK group. The increase in fumaric acid and citric acid contents suggested that the TCA cycle was disrupted, consequently disrupting the balance of energy metabolism in bacterial cells. D-Malic acid is a rare organic acid (Stern and Hegre 1966), and its excessive expression could lead to the abnormal growth of bacteria (Chinnici et al. 2005; Hopper et al. 1970; Martínez-Luque et al. 2001; Unden et al. 2016). The increase in cyanate content could lead to an increase in intracellular reactive oxygen species in bacterial cells, disrupt the balance of oxidative stress and eventually result in interference with the nitrogen metabolism pathway.

Validation of the pathway of resveratrol against S. typhimurium

According to the above metabolomic analysis results, the TCA cycle metabolic pathway of *S. typhimurium* was disrupted after resveratrol treatment. For further analysis, the

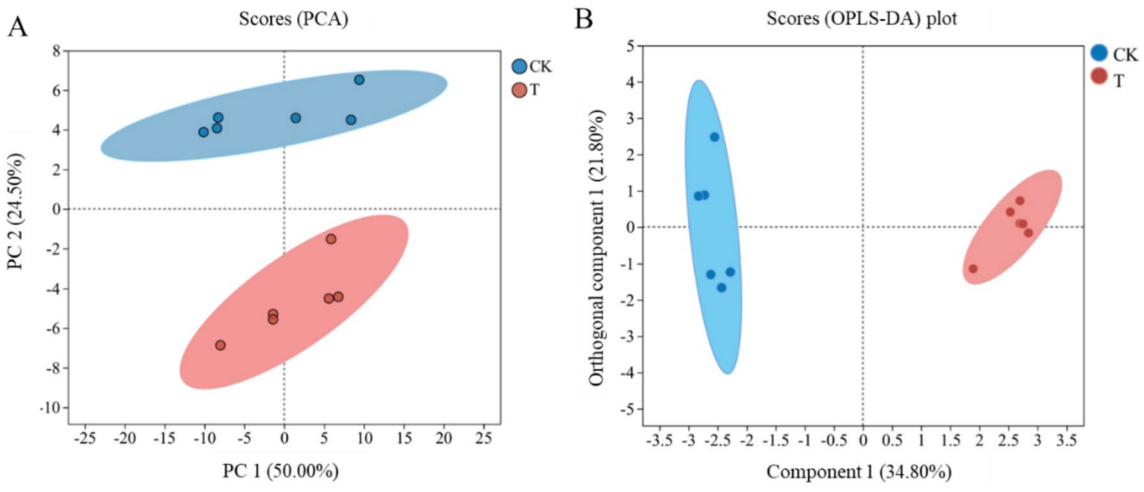

Fig. 7 Principal component (**A**) and orthogonal partial least square (**B**) analyses of metabolic profiles of *S. typhimurium* cells grown for 3 h at 37 °C in LB medium (control, blue) or in LB medium with 250 μg/mL resveratrol added (red)

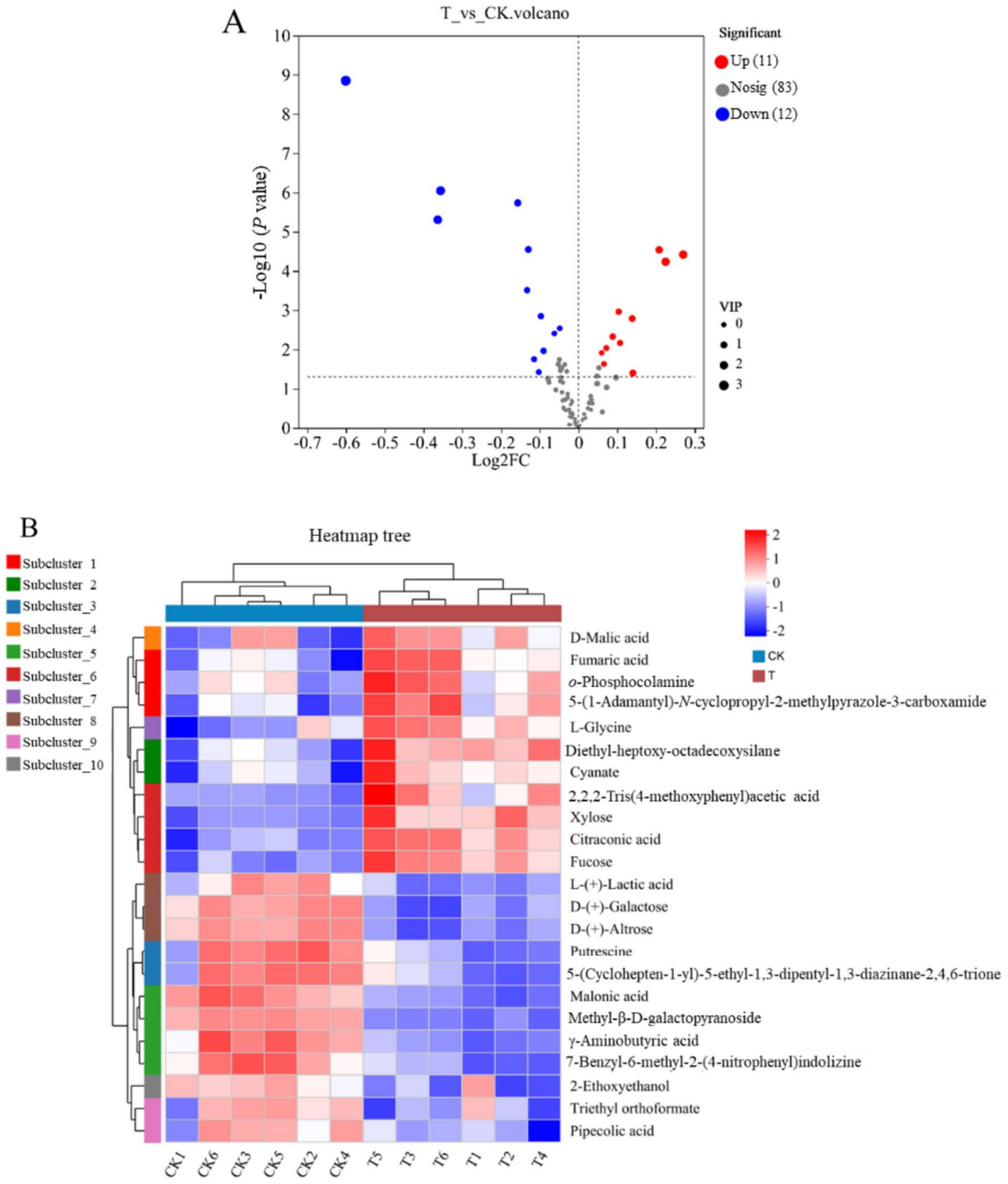

Fig. 8 Volcano plot (**A**) and heat map (**B**) identifying differentially produced metabolites by *S. typhimurium* cells grown for 3 h at 37 ℃ in LB medium with 250 μg/mL resveratrol added as compared with cells grown for 3 h at 37 ℃ LB medium (control). Upregulated metabolites in the Volcano plot are shown in red, downregulated metabolites in blue and metabolites with insignificant changes (nosing) in grey. In the heatmap, the redder the colour in the figure, the higher the expression abundance of the differential metabolites in the cells grown in presence of resveratrol

citric acid content, *cis*-aconitase activity and ATP content, which are key factors in the TCA cycle, were determined as in earlier bacterial studies (Noronha et al. 2017). When the concentration of resveratrol was 1/2 × MIC or 1 × MIC, the citric acid content increased significantly when compared with that in the CK group ($P < 0.01$) (Fig. 10A), which was consistent with the results of the metabolomics analysis. However, in contrast to those of the CK group, the intracellular *cis*-aconitase activity and ATP content of *S. typhimurium* significantly decreased ($P < 0.01$) after treatment with resveratrol at concentrations of 1/4 ×, 1/2 × and 1 × MIC (Fig. 10B, C).

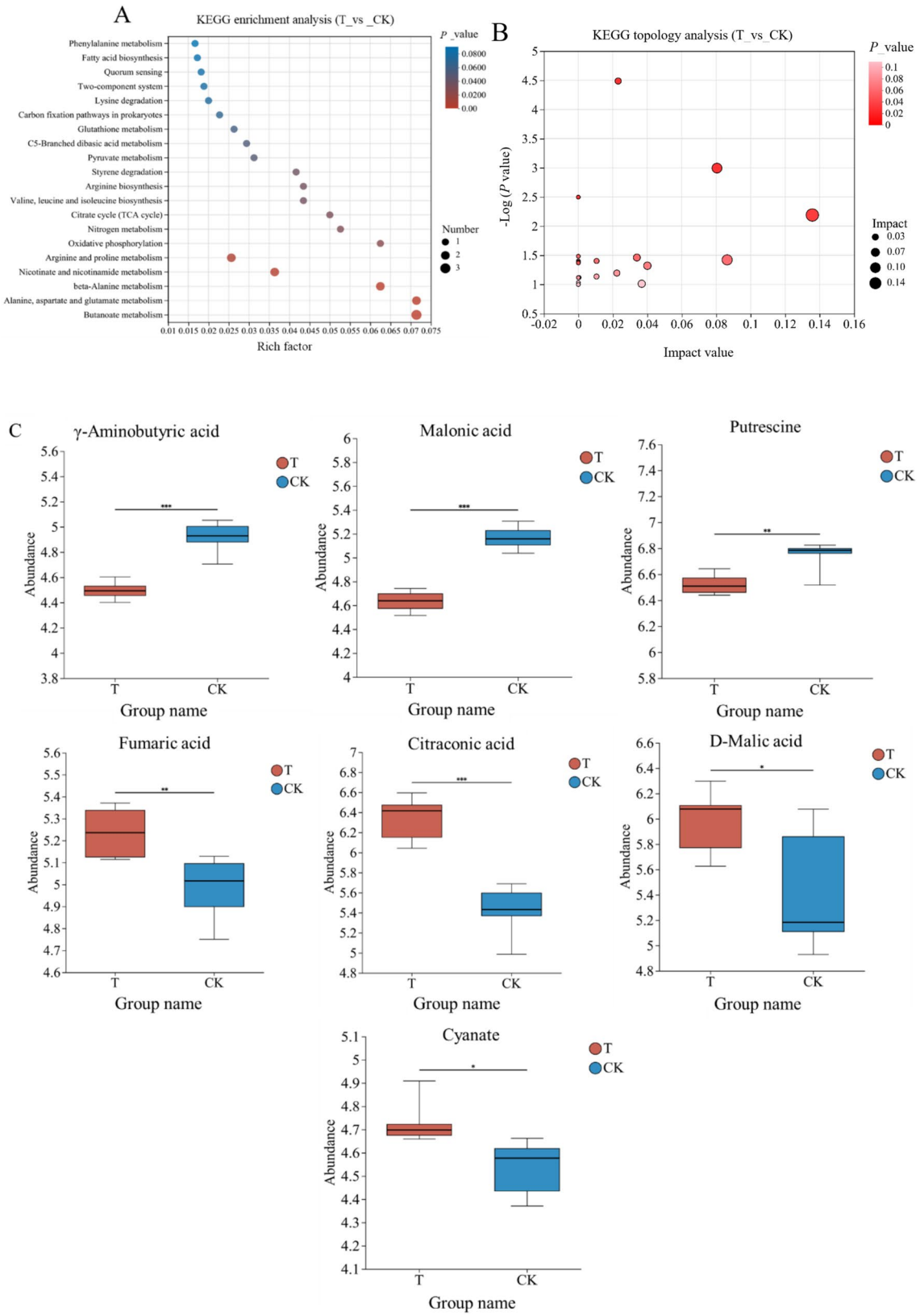
A
KEGG enrichment analysis (T_vs _CK)
Phenylalanine metabolism
Fatty acid biosynthesis
Quorum sensing
Two-component system
Lysine degradation
Carbon fixation pathways in prokaryotes
Glutathione metabolism
C5-Branched dibasic acid metabolism
Pyruvate metabolism
Styrene degradation
Arginine biosynthesis
Valine, leucine and isoleucine biosynthesis
Citrate cycle (TCA cycle)
Nitrogen metabolism
Oxidative phosphorylation
Arginine and proline metabolism
Nicotinate and nicotinamide metabolism
beta-Alanine metabolism
Alanine, aspartate and glutamate metabolism
Butanoate metabolism
Rich factor
P_value
Number
B
KEGG topology analysis (T_vs_CK)
-Log (P value)
Impact value
P_value
Impact
C
γ-Aminobutyric acid
Malonic acid
Putrescine
Fumaric acid
Citraconic acid
D-Malic acid
Cyanate
Abundance
Group name
T
CK

◂**Fig. 9** Bubble chart of KEGG enrichment pathways (**A**) and bubble chart of metabolic pathway analysis of differential metabolites (**B**) analysis identified the metabolic pathways involved in differential metabolites produced by *S. typhimurium* after 3 h growth in LB medium treated with 250 μg/mL resveratrol at 37 ℃ and after 3 h growth in LB medium (control) at 37 ℃. Different bubble colours indicate different *P* values of enrichment significance. The pathway was more important while the bubble was larger. Representative box plots of differential metabolite abundance values (**C**). The blue and red bars represent the blank control group and the 250 μg/mL resveratrol treated group, respectively. Abbreviations used: CK, untreated cells; T, cells treated with 250 μg/mL resveratrol. (* means $P<0.05$; ** means $P<0.01$; *** means $P<0.001$)

Discussion

In recent years, plant-derived extracts have become a hot topic in the field of antimicrobial research. Resveratrol, a polyphenolic compound, is widely found in many plants, such as grape seeds (Palomino et al. 2017). It is a green, natural and efficient antioxidant and a new antibacterial agent that has potential application value in the food industry and biomedicine field. In this study, resveratrol, which has better inhibitory activity against *S. typhimurium*, was screened from among 17 polyphenols and was subsequently used for further research on its antibacterial mechanism against *S. typhimurium* (Figs. 1 and 2). The results of the bacterial growth curves in this study also indicated that resveratrol, a natural product of plant origin, has a better inhibitory effect, which is similar to the effects of resveratrol on *Campylobacter* spp. and *Arcobacter butzleri* described in the study of Duarte et al. (2015) (Fig. 3).

Cell wall and cell membrane are protective barriers that can maintain cells in a stable metabolic environment and control transfer of substances in and out of cells (Lee and Lee 2017). When they are destroyed, substances inside bacteria, such as inorganic salt ions and proteins, leak into the culture medium (Yao et al. 2014). Therefore, a disturbance in the integrity of the cell wall and cell membrane can be reflected by a change in the substance content of the culture medium. According to the analysis of the cell membrane, cell wall permeability and bacterial micromorphological structure, protein, Na^+, K^+ and Mg^{2+} of *S. typhimurium* cells leaked to different degrees after treatment with different concentrations of resveratrol, and the enzymes related to ion transport, such as magnesium ion transport ATPase and potassium transport ATPase subunits, also changed. Among leaked out compounds, Mg^{2+} is an activator of various enzymes and participates in the establishment of transmembrane electron gradients, which not only can maintain the intracellular osmotic pressure but also stabilize cell membranes (Kanai et al. 2022). K^+ is also crucial for maintaining cellular osmotic pressure, and changes in amino acids can affect the synthesis of these enzymes and proteins, thereby affecting the transport of substances and transmembrane transport, preventing the growth of normal bacteria and ultimately achieving antibacterial effects (Abe et al. 2011).

Microbial metabolism is a complex and closely related process between metabolic substances (Joshua 2019). Metabolomic analysis revealed that resveratrol can affect multiple metabolic pathways by regulating the contents of sugars, organic acids, lipids, organic oxides and organic nitrides (Figs. 8, 9 and 10), especially several important metabolic pathways, such as glycolysis and the TCA cycle, thus leading to an imbalance in bacterial energy metabolism,

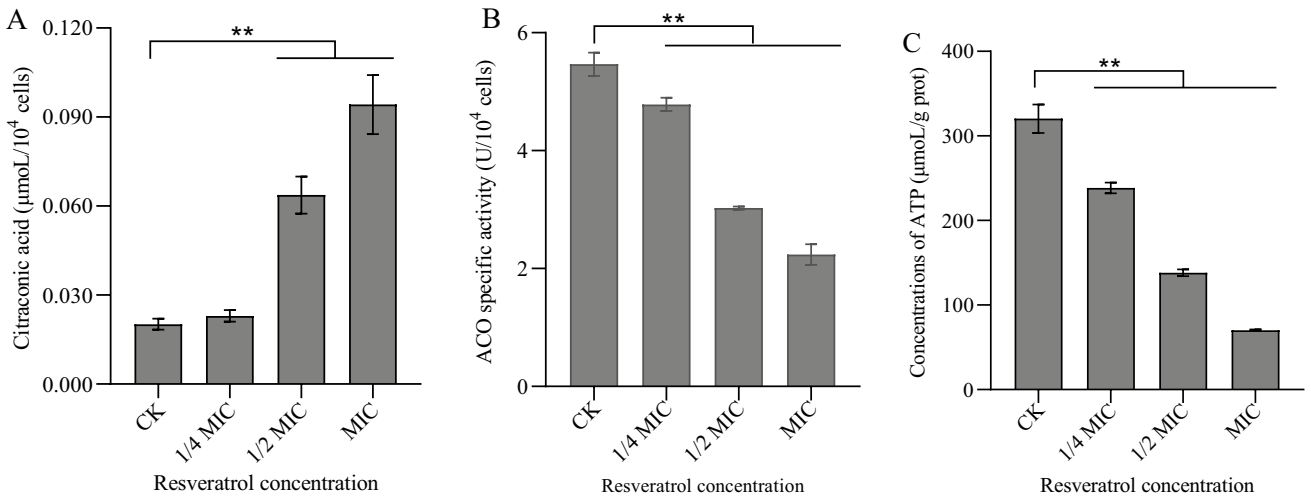

Fig. 10 Effect of resveratrol on the content of intracellular citraconic acid (**A**), activity of intracellular aconitase (**B**), and contents of intracellular ATP (**C**) in *S. typhimurium* cells grown for 3 h at 37 ℃ in LB medium. Abbreviations used: CK, blank control. (* means $P<0.05$; ** means $P<0.01$)

affecting nucleic acid synthesis, and damaging the cell wall and membrane. Finally, it can inhibit *S. typhimurium.*

In most bacterial infections, biofilms are the main virulence factor leading to infection (Zhang et al. 2020). Biofilms not only have functions such as material transport, information transmembrane transfer and energy conversion but also have unique physical forms that give them the ability to resist antibacterial drugs and host immune defence mechanisms (Yin et al. 2019). In this study, the effect of resveratrol on biofilm formation ability revealed that resveratrol significantly inhibited the biofilm formation of *S. typhimurium* in a concentration-dependent manner. The results of the metabolomics analysis further indicated that resveratrol may affect the formation of bacterial biofilms by inhibiting fatty acid metabolism, amino acid metabolism and energy metabolism in *S. typhimurium*, thus inhibiting bacterial growth (Shen et al. 2015; Wang et al. 2017).

At present, antibiotics are mainly used to control pathogenic bacteria in food (Salisbury et al. 2002). However, owing to the potential toxicity of synthetic substances, some researchers have focused on exploring active substances from plants in recent years (Zhu et al. 2019). In this study, we used metabolomics to analyse the metabolic pathways and metabolites that resveratrol inhibits in *S. typhimurium*. Studies have shown that resveratrol treatment can not only damage cell membranes but also cause metabolic disorders, resulting in the inhibition of bacterial growth. This provides a new direction for the use of resveratrol to inhibit the growth of bacteria in terms of small-molecule metabolites and is conducive to further research on the antibacterial mechanism of natural products. Combining the antibacterial effect of resveratrol and its own nutritional value, it has potential applications in medicine and food supplements.

Author contribution NW and QYY designed the study. CCN and ZZ conducted the experiments. CYY, HTR, LLC and GPZ analysed the data. CCN and QYY wrote the manuscript. All authors read and approved the manuscript.

Funding This work was supported by the Innovation and Ecological Support Special Project of Henan Province (HARS-22–05-Z1) and the Zhengzhou Key Laboratory of Nutrition and Healthy Food Project (KF20190426).

Data availability The datasets generated and analysed in this study are available from the corresponding author upon reasonable request.

Declarations

Ethical statement This article does not contain any studies with human participants or animals performed by any of the authors.

Competing interests The authors declare no competing interests.

References

Abe K, Tani K, Fujiyoshi Y (2011) Conformational rearrangement of gastric H^+, K^+-ATPase induced by an acid suppressant. Nat Commun 11(2):155–165

Biasutto L, Mattarei A, Azzolini M, La Spina M, Sassi N, Romio M, Paradisi C, Zoratti M (2017) Resveratrol derivatives as a pharmacological tool. Ann NY Acad Sci 1403(1):27–37

Cao S, Du R, Zhao F, Xiao H, Han Y, Zhou Z (2019) The mode of action of bacteriocin CHQS, a high antibacterial activity bacteriocin produced by *Enterococcus faecalis* TG2. Food Control 96:470–478

Chen M, Zhao Z, Meng H, Yu S (2017) The antibiotic activity and mechanisms of sugar beet (*Beta vulgaris*) molasses polyphenols against selected food-borne pathogens. LWT-Food Sci Technol 82:354–360

Chinnici F, Spinabelli U, Riponi C, Amati A (2005) Optimization of the determination of organic acids and sugars in fruit juices by ion-exclusion liquid chromatography. J Food Compos Anal 18(2–3):121–130

Dan W, Gao J, Li L, Xu Y, Wang J, Dai J (2021) Cellular and non-target metabolomics approaches to understand the antifungal activity of methylaervine against *Fusarium solani*. Bioorg Med Chem Lett 43:128068

Del Rio B, Redruello B, Ladero V, Fernandez M, Martin MC, Alvarez MA (2016) Putrescine production by *Lactococcus lactis* subsp. *cremoris* CECT 8666 is reduced by NaCl via a decrease in bacterial growth and the repression of the genes involved in putrescine production. Int J Food Microbiol 232:1–6

Deng W, Quan Y, Yang S, Guo L, Zhang X, Liu S, Chen S, Zhou K, He L, Li B (2018) Antibiotic resistance in *Salmonella* from retail foods of animal origin and its association with disinfectant and heavy metal resistance. Microb Drug Resist 24(6):782–791

Diao W-R, Hu Q-P, Zhang H, Xu J-G (2014) Chemical composition, antibacterial activity and mechanism of action of essential oil from seeds of fennel. Food Control 35(1):109–116

Diard M, Sellin ME, Dolowschiak T, Arnoldini M, Ackermann M, Hardt W (2014) Antibiotic treatment selects for cooperative virulence of *Salmonella typhimurium*. Curr Biol 24(17):2000–2005

Ding M-Z, Wang X, Yang Y, Yuan Y-J (2011) Metabolomic study of interactive effects of phenol, furfural, and acetic acid on *Saccharomyces cerevisiae*. OMICS 15(10):647–653

Duan J, Li M, Hao Z, Shen X, Liu L, Jin Y, Wang S, Guo Y, Yang L, Wang L (2018) Subinhibitory concentrations of resveratrol reduce alpha-hemolysin production in *Staphylococcus aureus* isolates by downregulating *saeRS*. Emerg Microbes Infec 7(1):1–10

Duarte A, Alves AC, Ferreira S, Silva F, Domingues F (2015) Resveratrol inclusion complexes: antibacterial and anti-biofilm activity

against *Campylobacter* spp. and *Arcobacter butzleri*. Food Res Int 77:244–250
Ebani VV, Nardoni S, Bertelloni F, Tosi G, Massi P, Pistelli L, Mancianti F (2019) In vitro antimicrobial activity of essential oils against *Salmonella enterica* serotypes Enteritidis and Typhimurium strains isolated from poultry. Molecules 24(5):900
Guanlin W, Jinhua T (2006) Bacteriostatic action and mechanism of *Sophora flavescens* Ait on *Escherichia coli* 01 C84010. Sci Agric Sin 39:1018–1024
Hameed ASH, Karthikeyan C, Ahamed AP, Thajuddin N, Alharbi NS, Alharbi SA, Ravi G (2016) In vitro antibacterial activity of ZnO and Nd doped ZnO nanoparticles against ESBL producing *Escherichia coli* and *Klebsiella pneumoniae*. Sci Rep-UK 6(1):1–1
Hopper D, Chapman P, Dagley S (1970) Metabolism of L-malate and D-malate by a species of *Pseudomonas*. J Bacteriol 104(3):1197–1202
Hyldgaard M, Mygind T, Vad BS, Stenvang M, Otzen DE, Meyer RLJA (2014) The antimicrobial mechanism of action of ε-poly-L-lysine. Applied Environ Microbiol 80(24):7758–7770
Joshua CJ (2019) Metabolomics: a microbial physiology and metabolism perspective. Methods Mol Biol 1859:71–94
Kanai R, Cornelius F, Vilsen B, Toyoshima C (2022) Cryoelectron microscopy of Na^+, ^{K}+-ATPase in the two E2P states with and without cardiotonic steroids. Proc Natl Acad Sci 119(15):e2123226119
Koch J, Steinert M, Koch S, Soeberdt M, Knie U, Abels C, Luger T, Loser K (2019) A chemically modified derivative of the anti-inflammatory tripeptide KdPT (WOL074-009) ameliorates ongoing psoriasis and colitis. Exp Dermatol 25(4):1867–1890
Lee W, Lee DG (2017) Resveratrol induces membrane and DNA disruption via pro-oxidant activity against *Salmonella typhimurium*. Biochem Bioph Res Co 489(2):228–234
Lewandowski Z, Beyenal H, Myers J, Stookey D (2007) The effect of detachment on biofilm structure and activity:the oscillating pattern of biofilm accumulation. Water Sci Technol 55(8):429–436
Li J, Wu T, Peng W, Zhu Y (2020) Effects of resveratrol on cariogenic virulence properties of *Streptococcus mutans*. BMC Microbiol 20(1):1–11
Liang X, Dickman MB, Becker DF (2014) Proline biosynthesis is required for endoplasmic reticulum stress tolerance in *Saccharomyces cerevisiae*. J Biol Chem 289(40):27794–27806
Liu G, Ren G, Zhao L, Cheng L, Wang C, Sun B (2017) Antibacterial activity and mechanism of bifidocin A against *Listeria monocytogenes*. Food Control 73:854–861
Liu M, Feng M, Yang K, Cao Y, Zhang J, Xu J, Hernández SH, Wei X, Fan M (2020) Transcriptomic and metabolomic analyses reveal antibacterial mechanism of astringent persimmon tannin against methicillin-resistant *Staphylococcus aureus* isolated from pork. Food Chem 309:125692
Lv F, Liang H, Yuan Q, Li C (2011) In vitro antimicrobial effects and mechanism of action of selected plant essential oil combinations against four food-related microorganisms. Food Res Int 44(9):3057–3064
Marino A, Santoro G, Spataro F, Lauriano ER, Pergolizzi S, Cimino F, Speciale A, Nostro A, Bisignano G, Dugo G (2013) Resveratrol role in *Staphylococcus aureus*-induced corneal inflammation. Pathog Dis 68(2):61–64
Martínez-Luque M, Castillo F, Blasco R (2001) Assimilation of D-malate by *Rhodobacter capsulatus* E1F1. Curr Microbiol 43(3):154–157
Mezal EH, Stefanova R, Khan A (2013) Isolation and molecular characterization of *Salmonella enterica* serovar Javiana from food, environmental and clinical samples. Int J Food Microbiol 164(1):113–118
Natera V, Sobrevals L, Fabra A, Castro S (2006) Glutamate is involved in acid stress response in *Bradyrhizobium* sp. SEMIA 6144 (*Arachis hypogaea* L.) microsymbiont. Curr Microbiol 53(6):479–482
Niven GW, Miles CA, Mackey BM (1999) The effects of hydrostatic pressure on ribosome conformation in *Escherichia coli*: an in vivo study using differential scanning calorimetry. Microbiology 145(2):419–425
Noronha SB, Yeh HJ, Spande TF, Shiloach J (2017) Investigation of the TCA cycle and the glyoxylate shunt in *Escherichia coli* BL21 and JM109 using 13C-NMR/MS. Biotechnol Bioeng 68(3):316–327
Novo D, Perlmutter NG, Hunt RH, Shapiro H (1999) Accurate flow cytometric membrane potential measurement in bacteria using diethyloxacarbocyanine and a ratiometric technique. Cytometry 35(1):55–63
Olaimat AN, Holley RA (2012) Factors influencing the microbial safety of fresh produce: a review. Food Microbiol 32(1):1–19
Palomino O, Gómez-Serranillos MP, Slowing K, Carretero E, Villar A (2017) Study of polyphenols in grape berries by reversed-phase high-performance liquid chromatography. J Chromatogr A 870(1–2):449–451
Patra JK, Das G, Choi JW, Baek K (2016) Antibacterial effects of pyrolysis oil against *Salmonella typhimurium* and *Escherichia coli*. Foodborne Pathog Dis 13(1):13–20
Renoz F, Noël C, Errachid A, Foray V, Hance T (2015) Infection dynamic of symbiotic bacteria in the pea aphid acyrthosiphon pisum gut and host immune response at the early steps in the infection process. PLoS One 10(3):e0122099
Salisbury JG, Nicholls TJ, Lammerding AM, Turnidge J, Nunn MJ (2002) A risk analysis framework for the long-term management of antibiotic resistance in food-producing animals. Int J Antimicrob Ag 20(3):153–164
Scallan E, Hoekstra RM, Angulo FJ, Tauxe RV, Widdowson M-A, Roy SL, Jones JL, Griffin PM (2011) Foodborne illness acquired in the United States-major pathogens. Emerg Infect Dis 17(1):7
Shen S, Zhang T, Yuan Y, Lin S, Xu J, Ye H (2015) Effects of cinnamaldehyde on *Escherichia coli* and *Staphylococcus aureus* membrane. Food Control 47:196–202
Simon S, Trost E, Bender J, Fuchs S, Malorny B, Rabsch W, Prager R, Tietze E, Flieger A (2018) Evaluation of WGS based approaches for investigating a food-borne outbreak caused by *Salmonella enterica* serovar Derby in Germany. Food Microbiol 71:46–54
Singh AK, Vinayak M (2016) Antinociceptive effect of resveratrol during inflammatory hyperalgesia via differential regulation of pro-inflammatory mediators. PTR 30(7):1164–1171
Singh AP, Singh R, Verma SS, Rai V, Kaschula CH, Maiti P, Gupta SC (2019) Health benefits of resveratrol: evidence from clinical studies. Med Res Rev 39(5):1851–1891
Stern JR, Hegre C (1966) Inducible D-malic enzyme in *Escherichia coli*. Nature 212(5070):1611–1612
Stojković D, Petrović J, Soković M, Glamočlija J, Kukić-Marković J, Petrović S (2013) In situ antioxidant and antimicrobial activities of naturally occurring caffeic acid, *p*-coumaric acid and rutin, using food systems. J Sci Food Agr 93(13):3205–3208
Sun X-H, Zhou T-T, Wei C-H, Lan W-Q, Zhao Y, Pan Y-J, Wu V-C (2018) Antibacterial effect and mechanism of anthocyanin rich Chinese wild blueberry extract on various foodborne pathogens. Food Control 94:155–161
Takagi H, Iwamoto F, Nakamori S (1997) Isolation of freeze-tolerant laboratory strains of *Saccharomyces cerevisiae* from proline-analogue-resistant mutants. Appl Microbiol Biotechnol 47(4):405–411
Unden G, Strecker A, Kleefeld A, Kim O (2016) C4-dicarboxylate utilization in aerobic and anaerobic growth. Ecosal Plus 7(1):0021. https://doi.org/10.1128/ecosalplus.esp-0021-2015
Vasudevan P, Nair MKM, Annamalai T, Venkitanarayanan KS (2003) Phenotypic and genotypic characterization of bovine mastitis

isolates of *Staphylococcus aureus* for biofilm formation. Vet Microbiol 92(1–2):179–185

Wang C, Chang T, Yang H, Cui M (2014) Surface physiological changes induced by lactic acid on pathogens in consideration of pKa and pH. Food Control 46:525–531

Wang F, Wei F, Song C, Jiang B, Tian S, Yi J, Yu C, Song Z, Sun L, Bao Y (2017) *Dodartia orientalis* L. essential oil exerts antibacterial activity by mechanisms of disrupting cell structure and resisting biofilm. Ind Crop Prod 109:358–366

Wang L, Zhao X, Xia X, Zhu C, Zhang H, Qin W, Xu Y, Hang B, Sun Y, Chen S (2019) Inhibitory effects of antimicrobial peptide JH-3 on *Salmonella enterica* serovar Typhimurium strain CVCC541 infection-induced inflammatory cytokine release and apoptosis in RAW264. 7 cells. Molecules 24(3):596

Wang Y, Liu B, Zhang J, Sun L, Wen W, Fan Q, Yi L (2019) Infection with soda mutant of *S. typhimurium* leads to up-regulation of autophagy in Raw264·7 macrophages. Lett Appl Microbiol 69(1):11–15

Weerakkody NS, Caffin N, Turner MS, Dykes GA (2010) In vitro antimicrobial activity of less-utilized spice and herb extracts against selected food-borne bacteria. Food Control 21(10):1408–1414

West TP, O'Donovan GA (2017) Repression of cytosine deaminase by pyrimidines in *Salmonella typhimurium*. J Bacteriol 149(3):1171–1174

Westerhuis JA, van Velzen EJ, Hoefsloot HC, Smilde AK (2010) Multivariate paired data analysis: multilevel PLSDA versus OPLSDA. Metabolomics 6:119–128

Wu F-S, Gibbs TT, Farb DH (1993) Dual activation of GABAA and glycine receptors by β-alanine: inverse modulation by progesterone and 5α-pregnan-3α-ol-20-one. Eur J Pharmacol 246(3):239–246

Xu J-G, Liu T, Hu Q-P, Cao X-M (2016) Chemical composition, antibacterial properties and mechanism of action of essential oil from clove buds against *Staphylococcus aureus*. Molecules 21(9):1194

Yao C, Li X, Bi W, Jiang C (2014) Relationship between membrane damage, leakage of intracellular compounds, and inactivation of *Escherichia coli* treated by pressurized CO_2. J Basic Microbiol 54(8):858–865

Yi L, Dang J, Zhang L, Wu Y, Liu B, Lü X (2016) Purification, characterization and bactericidal mechanism of a broad spectrum bacteriocin with antimicrobial activity against multidrug-resistant strains produced by *Lactobacillus coryniformis* XN8. Food Control 67:53–62

Yin W, Wang Y, Liu L, He J (2019) Biofilms: the microbial "protective clothing" in extreme environments. Int J Mol Sci 20(14):3423–3430

Zhang D, Gan R-Y, Zhang J-R, Farha AK, Li H-B, Zhu F, Wang X-H, Corke H (2020) Antivirulence properties and related mechanisms of spice essential oils: a comprehensive review. Compr Rev Food Sci Food Saf 19(3):1018–1055

Zhu J-J, Yang J-X, Fang H-L, Zhang A-L, Feng Y, Shao Q-S (2019) Antibacterial and antifungal activities of different polar extracts from *Anoectochilus roxburghii*. Pak J Pharm Sci 32(6):2745–2751